

Entanglement Entropy Near Kondo-Destruction Quantum Critical Points

J. H. Pixley,^{1,2} Tathagata Chowdhury,³ M. T. Miecnikowski,^{3,4,*}
Jaimie Stephens,^{3,5} Christopher Wagner,³ and Kevin Ingersent³

¹*Condensed Matter Theory Center and the Joint Quantum Institute,
Department of Physics, University of Maryland, College Park, Maryland 20742-4111, USA*

²*Department of Physics and Astronomy, Rice University, Houston, Texas, 77005, USA*

³*Department of Physics, University of Florida, Gainesville, Florida 32611-8440, USA*

⁴*Department of Applied Physics and Applied Mathematics, Columbia University,
500 W. 120th St., Mudd 200, MC 4701 New York, NY 10027*

⁵*Department of Physical and Environmental Sciences,
Colorado Mesa University, Grand Junction, Colorado 81501-3122, USA*

(Dated: July 19, 2018)

We study the impurity entanglement entropy S_e in quantum impurity models that feature a Kondo-destruction quantum critical point (QCP) arising from a pseudogap in the conduction-band density of states or from coupling to a bosonic bath. On the local-moment (Kondo-destroyed) side of the QCP, the entanglement entropy contains a critical component that can be related to the order parameter characterizing the quantum phase transition. In Kondo models describing a spin- S_{imp} , S_e assumes its maximal value of $\ln(2S_{\text{imp}} + 1)$ at the QCP and throughout the Kondo phase, independent of features such as particle-hole symmetry and under- or over-screening. In Anderson models, S_e is nonuniversal at the QCP, and at particle-hole symmetry, rises monotonically on passage from the local-moment phase to the Kondo phase; breaking this symmetry can lead to a cusp peak in S_e due to a divergent charge susceptibility at the QCP. Implications of these results for quantum critical systems and quantum dots are discussed.

PACS numbers: 71.10.Hf, 71.27.+a, 75.20.Hr

I. INTRODUCTION

Entanglement entropy has emerged as a powerful tool for quantifying correlations in pure and mixed states of quantum many-body systems, and particularly for characterizing unconventional ground states. In cases where a local order parameter is not sufficient, the entanglement entropy S_e [defined in Eq. (1) below] can be used to identify nontrivial topological order [1]. It has been established[2] that S_e exhibits nontrivial scaling in the vicinity of continuous zero-temperature phase transitions, i.e., at quantum critical points [3]. From an information perspective, entanglement is a generic feature of quantum-mechanical systems that may be used for storing information as well as for quantum computation [4].

Due to the nonlocality of entanglement entropy, there are relatively few interacting problems where it has proved possible to accurately determine S_e , particularly in the vicinity of quantum phase transitions. In this context, quantum impurity problems have the advantage that they can be solved reliably via a number of well-established techniques. Conformal field theory [5], the density-matrix renormalization group [5], and the numerical renormalization group [6] have all been used to calculate entanglement entropy in the Kondo and spin-boson models. Quantum impurity models therefore provide a natural setting for systematic study of the interplay

between quantum criticality and entanglement entropy. For example, it has been established using the numerical renormalization-group (NRG) method [6–8] that S_e exhibits a cusp peak at the quantum critical point (QCP) that separates the localized and delocalized phases of the sub-ohmic spin-boson model. Whether or not a cusp peak in S_e at the QCP is a generic feature of continuous impurity quantum phase transitions is an open and intriguing question.

The Kondo and Anderson impurity models [9], originally shown to describe the many-body screening of the magnetic moments of dilute magnetic impurities in non-magnetic metals, have now found applications in other contexts, including but not limited to the physics of heavy f -electron systems and transport through quantum dots. Here, we study variants of these models that exhibit critical destruction of the Kondo effect, where Kondo screening is suppressed at a second-order quantum phase arising from the presence of a pseudogap in the conduction-band density of states around the Fermi energy [10–18] and/or an additional coupling of the impurity to a bosonic environment [19–25]. Kondo destruction QCPs in the Bose-Fermi Kondo model have been proposed to describe anomalous quantum criticality in heavy fermion metals [26, 27] and non-equilibrium criticality in a quantum dot with ferromagnetic leads [28]. Pseudogap Kondo and Anderson models have been used to study nonmagnetic impurities in d -wave superconductors [29] and in graphene [30]. It has also been shown that tuning a double-quantum-dot system can produce a pseudogap in the effective density of states [31, 32].

* Present address: Department of Physics, University of Colorado, Libby Drive, Boulder, Colorado 80302-0390, USA

While each of these models have been studied in the past, little is known about their entanglement entropy properties, a gap that this work aims to fill.

By combining analytic and NRG calculations, we establish that the entanglement entropy contains a critical component in the vicinity of these Kondo-destruction QCPs. In Kondo models with a spin- S_{imp} impurity moment, we show that S_e takes its maximal value of $\ln(2S_{\text{imp}} + 1)$ at the QCP and throughout the Kondo phase, and decreases in a power-law fashion on entry into the Kondo-destroyed or local-moment phase. These behaviors highlight some differences between the Kondo and spin-boson models. In pseudogap Anderson models, we show that charge fluctuations lead S_e to take a nonuniversal value at the quantum phase transition. At particle-hole symmetry, S_e always increases with increasing impurity-band hybridization Γ and is therefore never peaked at the quantum phase transition. Away from particle-hole symmetry, S_e can vary non-monotonically with Γ , and in some cases exhibits a cusp peak at the QCP.

The remainder of this paper is organized as follows: Section II reviews general characteristics of the entanglement entropy and summarizes the universal behaviors that we find at Kondo-destruction QCPs. Detailed analysis of various Kondo models and Anderson models is presented in Secs. III and IV, respectively. We discuss our results in Sec. V and conclude in Sec. VI.

II. GENERAL CONSIDERATIONS

Entanglement entropy captures the degree of quantum nonlocality in the ground-state wave function. Specifically, it is a property associated with a partition of the system into two regions A and B that effectively “cuts” the ground state along the boundary between the regions. Upon tracing the system’s density operator $\hat{\rho}$ over region B , one obtains the reduced density operator in region A , $\hat{\rho}_A = \text{Tr}_B \hat{\rho}$. Similarly, one can trace over region A to obtain $\hat{\rho}_B = \text{Tr}_A \hat{\rho}$. The entanglement entropy is the von Neumann entropy of $\hat{\rho}_A$ or $\hat{\rho}_B$, i.e.,

$$S_e(A|B) = -\text{Tr}_A(\hat{\rho}_A \ln \hat{\rho}_A) \equiv -\text{Tr}_B(\hat{\rho}_B \ln \hat{\rho}_B), \quad (1)$$

which measures the extent to which region A is entangled with region B .

In quantum impurity problems, the entanglement entropy between the impurity and the rest of the system is defined by taking region A to contain solely the impurity degrees of freedom, while region B describes the host (i.e., the rest of the system), as shown schematically in Fig. 1. Upon tracing out the host, we obtain the impurity reduced density operator $\hat{\rho}_{\text{imp}}$ acting in a vector space of dimension d_{imp} . Equation (1) then gives the impurity

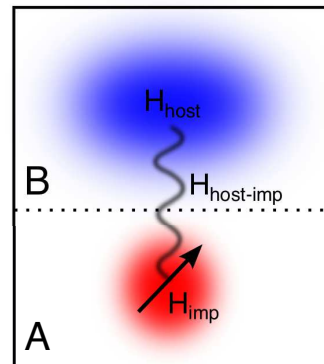


FIG. 1. (Color online) Schematic representation of the model Hamiltonians considered in this work. The impurity degrees of freedom H_{imp} are coupled via $H_{\text{host-imp}}$ (wavy line) to the bath degrees of freedom H_{host} . We trace out region B , and determine the entanglement entropy of region A .

entanglement entropy [6, 7]

$$S_e = - \sum_{i=1}^{d_{\text{imp}}} p_i \ln p_i, \quad (2)$$

where $\{p_i\}$ is the set of eigenvalues of $\hat{\rho}_{\text{imp}}$. The corresponding eigenstates $\{|i\rangle\}$ must respect the system’s symmetries, a constraint that allows the eigenvalues p_i to be expressed in terms of expectation values of impurity operators that can readily be calculated using the NRG. Since the host degrees of freedom have been completely traced out, the impurity entanglement entropy measures only the entanglement between the impurity and the host as a whole. Details of the host—such as the number, dispersion, and any internal interactions of the conduction bands and/or the bosonic baths—influence S_e only insofar as they affect the impurity matrix elements that determine the eigenvalues of $\hat{\rho}_{\text{imp}}$.

For a ground state of product form $|\psi\rangle = |\phi\rangle_{\text{imp}} \otimes |\chi\rangle_{\text{host}}$, one can choose $p_1 = 1$ and $p_i = 0$ for all $i > 1$, implying that $S_e = 0$. At the other extreme, a state of maximal entanglement between the impurity and its host is described by $p_i = 1/d_{\text{imp}}$ for all i , leading to $S_e = \ln d_{\text{imp}}$.

A complication arises if the system is not in a pure state, as is likely to be the case when there is ground-state degeneracy. For example, in the trivial limit where the impurity and the host are decoupled, n -fold degeneracy of the impurity ground state results in $\hat{\rho}_{\text{imp}}$ having n values $p_i = 1/n$ and $d_{\text{imp}} - n$ values $p_i = 0$, implying that $S_e = \ln n$. In order to avoid such misleading indications of entanglement, it is necessary to break the ground-state degeneracy of the impurity to obtain a pure state.

In the present work, where we treat magnetic impurities, the ground-state degeneracy can be lifted by the application of an infinitesimal local magnetic field h_{loc} that couples solely to the impurity through a Hamiltonian term $h_{\text{loc}} S_{\text{imp}}^z$, where S_{imp} is the impurity spin op-

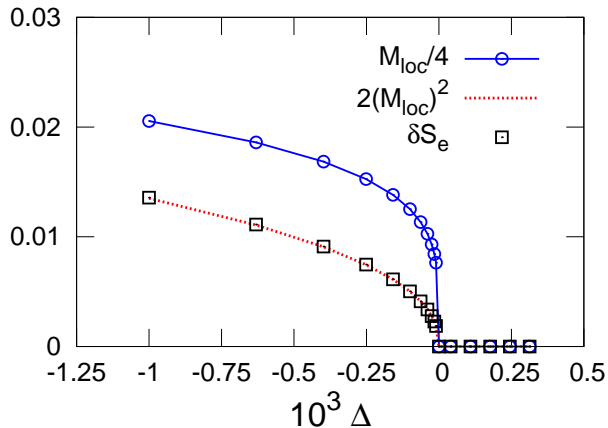


FIG. 2. (Color online) Order parameter $M_{\text{loc}}(\Delta, h_{\text{loc}} = 0^+)$ and spontaneous-symmetry-breaking part of the entanglement entropy $\delta S_e(\Delta)$ vs distance $\Delta = (J - J_c)/J_c$ from the quantum critical point of the Bose-Fermi Kondo model with an Ising-symmetry coupling $K_0 g = 7.5$ between an impurity spin $S_{\text{imp}} = \frac{1}{2}$ and a bosonic bath with exponent $s = 0.8$. On approach to the QCP from the local-moment phase ($\Delta < 0$), δS_e vanishes like $2M_{\text{loc}}^2$.

erator and the Landé g factor and the Bohr magneton have both been set to unity. For this reason, we consider a two-parameter function $S_e(x, h_{\text{loc}})$, where x is a non-thermal, nonmagnetic parameter that tunes the system through a QCP at $x = x_c$. In many cases, we employ a reduced variable $\Delta = (x - x_c)/x_c$ such that the QCP is located at $\Delta = 0$. It also proves convenient to define the local-field-dependent part of the entanglement entropy (note the sign)

$$\delta S_e(x, h_{\text{loc}}) = S_e(x, 0) - S_e(x, h_{\text{loc}}), \quad (3)$$

and to introduce the shorthand notations

$$S_e^+(x) = S_e(x, h_{\text{loc}} = 0^+), \quad (4a)$$

$$\delta S_e(x) = \delta S_e(x, h_{\text{loc}} = 0^+) \quad (4b)$$

representing, respectively, the degeneracy-lifted entanglement entropy and the reduction in entanglement entropy due to spontaneous symmetry breaking.

In Secs. III and IV, we report results for the entanglement entropy in several quantum impurity Hamiltonians of the general form

$$H = H_{\text{host}} + H_{\text{imp}} + H_{\text{host-imp}} \quad (5)$$

where H_{host} describes one or more fermionic bands as well as, possibly, a bosonic bath. The term H_{imp} describes the isolated impurity, and $H_{\text{host-imp}}$ accounts for the coupling between the host and the impurity. The fermionic bands are assumed to have a dispersion $\epsilon_{\mathbf{k}}$ giving rise to an idealized density of states

$$\rho_c(\epsilon) = N_k^{-1} \sum_{\mathbf{k}} \delta(\epsilon - \epsilon_{\mathbf{k}}) = \rho_0 |\epsilon/D|^r \Theta(D - |\epsilon|), \quad (6)$$

where N_k is number of distinct \mathbf{k} values, $\Theta(x)$ is the Heaviside function, D is the half-bandwidth, and r is a band exponent. QCPs arise in pure-fermionic Kondo and Anderson models in cases $0 < r < 1$ describing pseudogapped hosts in which $\rho_c(\epsilon)$ vanishes in a sub-linear fashion at the Fermi energy $\epsilon_F = 0$.

Another route to impurity QCPs is competition between fermionic and bosonic environments for control of an impurity degree of freedom. Below we consider models with a metallic fermionic density of states described by Eq. (6) with $r = 0$ as well as a bosonic bath assumed to have a dispersion $\omega_{\mathbf{q}}$ that gives rise to a density of states

$$\rho_\phi(\omega) = N_q^{-1} \sum_{\mathbf{q}} \delta(\omega - \omega_{\mathbf{q}}) = K_0^2 \omega_c^{1-s} |\omega|^s \Theta(\omega) \Theta(\omega_c - \omega), \quad (7)$$

where N_q is the number of distinct \mathbf{q} modes, ω_c is an ultra-violet frequency cutoff, and s is a bath exponent assumed to lie in the range $1/2 < s < 1$.

In all of the models we consider it has been established that a QCP separates a Kondo phase (corresponding to tuning parameter values $\Delta > 0$) from a local-moment phase (spanning $\Delta < 0$), in which the Kondo effect is destroyed. The models include ones in which the Kondo phase exhibits exact screening, over-screening, or under-screening of the impurity spin. In each case an appropriate order parameter for the quantum phase transition is the $h_{\text{loc}} \rightarrow 0^+$ limit of the local magnetization $M_{\text{loc}}(\Delta, h_{\text{loc}}) = -\lim_{T \rightarrow 0} \langle S_{\text{imp}}^z \rangle$, which vanishes throughout the Kondo phase, and in the local-moment phase close to the QCP obeys

$$M_{\text{loc}}(\Delta, h_{\text{loc}} = 0^+) \propto (-\Delta)^\beta, \quad (8)$$

where β is the order-parameter exponent. At the critical value of the tuning parameter, the local magnetization satisfies

$$M_{\text{loc}}(\Delta = 0, h_{\text{loc}}) \propto |h_{\text{loc}}|^{1/\delta}, \quad (9)$$

where δ is another critical exponent.

We show very generally—independent of features such as particle-hole symmetry or asymmetry, the degree of impurity charge fluctuations, whether the Kondo phase involves exact, over-, or under-screening, and the presence or absence of competition between fermionic bands and bosonic baths—that upon approach to the QCP from the local-moment side, the entanglement entropy satisfies

$$\delta S_e(\Delta, h_{\text{loc}}) = a M_{\text{loc}}^2, \quad (10)$$

where a is a constant that depends on details of the model. This connection is illustrated in Fig. 2, which shows the variation of $M_{\text{loc}}(\Delta, h_{\text{loc}} = 0^+)$ and $\delta S_e(\Delta)$ with reduced Kondo coupling $\Delta = (J - J_c)/J_c$ in the Ising-symmetry Bose-Fermi Kondo model [defined in Eqs. (14) below], for which we show that $a = 2$.

When combined with Eqs. (8) and (9), Eq. (10) implies that

$$\delta S_e(\Delta < 0, h_{\text{loc}} = 0^+) \propto (-\Delta)^{\beta_e}, \quad (11a)$$

$$\delta S_e(\Delta = 0, h_{\text{loc}}) \propto |h_{\text{loc}}|^{1/\delta_e}, \quad (11b)$$

with

$$\beta_e = 2\beta, \quad (12a)$$

$$1/\delta_e = 2/\delta, \quad (12b)$$

scaling relations that are demonstrated explicitly in the numerical results presented below.

We solve the quantum impurity problems introduced above using the NRG [33, 34] as adapted to treat quantum impurity problems involving a pseudogapped fermionic density of states [11, 12] and/or a sub-ohmic bath of bosons [23, 25, 35, 36]. The impurity entanglement entropy is found via Eq. (2) using reduced density matrix eigenvalues p_i expressed in terms of expectation values (converged for large NRG iteration numbers corresponding to asymptotically low temperatures) of certain impurity operators specified in the sections that follow. We use a Wilson discretization parameter $3 \leq \Lambda \leq 9$, a range that has been shown previously to provide an accurate account of the critical exponents [13, 23–25]. Close to the QCP, we find it necessary to employ quadruple-precision floating-point calculations in order to accurately resolve the entanglement entropy, and in particular, the value of $\delta S_e(\Delta)$ defined in Eq. (4b).

III. KONDO AND BOSE-FERMI KONDO MODELS

The Kondo models under consideration are described by Hamiltonians of the form of Eq. (5) with

$$H_{\text{host}} = \sum_{\mathbf{k}, \sigma, \alpha} \epsilon_{\mathbf{k}} c_{\mathbf{k}\sigma\alpha}^\dagger c_{\mathbf{k}\sigma\alpha}, \quad (13a)$$

$$H_{\text{imp}} = h_{\text{loc}} S_{\text{imp}}^z, \quad (13b)$$

$$H_{\text{host-imp}} = J \mathbf{S}_{\text{imp}} \cdot \sum_{\sigma, \sigma', \alpha} c_{0\sigma\alpha}^\dagger \frac{1}{2} \boldsymbol{\sigma}_{\sigma\sigma'} c_{0\sigma'\alpha} + W \sum_{\sigma, \alpha} c_{0\sigma\alpha}^\dagger c_{0\sigma\alpha}, \quad (13c)$$

where $c_{\mathbf{k}\sigma\alpha}$ destroys a conduction electron of wave vector \mathbf{k} , spin z component $\sigma = \pm \frac{1}{2} \equiv \uparrow, \downarrow$, channel index $\alpha \in \{1, \dots, K\}$, and energy $\epsilon_{\mathbf{k}}$ satisfying Eq. (6); $c_{0\sigma\alpha} = N_k^{-1/2} \sum_{\mathbf{k}} c_{\mathbf{k}\sigma\alpha}$ destroys an electron of spin z component σ and channel index α at the impurity site; and \mathbf{S}_{imp} is the spin operator for a spin- S_{imp} impurity. The host-impurity coupling is characterized by an anti-ferromagnetic exchange $J > 0$ and a potential scattering W .

In Sec. III A we consider pseudogap Kondo models described by Eqs. (5) and (13) with an impurity spin

$S_{\text{imp}} = \frac{1}{2}$ and channel numbers $K = 1$ (exactly screened impurity) and $K = 2$ (overscreened impurity). We also consider the (one-channel, $S_{\text{imp}} = \frac{1}{2}$) Ising-symmetry Bose-Fermi Kondo model described by Eq. (5) with

$$H_{\text{host}} = \sum_{\mathbf{k}, \sigma, \alpha} \epsilon_{\mathbf{k}} c_{\mathbf{k}\sigma\alpha}^\dagger c_{\mathbf{k}\sigma\alpha} + \sum_{\mathbf{q}} \omega_{\mathbf{q}} \phi_{\mathbf{q}}^\dagger \phi_{\mathbf{q}}, \quad (14a)$$

$$H_{\text{imp}} = h_{\text{loc}} S_{\text{imp}}^z \quad (14b)$$

$$H_{\text{host-imp}} = J \mathbf{S}_{\text{imp}} \cdot \sum_{\sigma, \sigma', \alpha} c_{0\sigma\alpha}^\dagger \frac{1}{2} \boldsymbol{\sigma}_{\sigma\sigma'} c_{0\sigma'\alpha} + W \sum_{\sigma, \alpha} c_{0\sigma\alpha}^\dagger c_{0\sigma\alpha} + g S_{\text{imp}}^z \frac{1}{\sqrt{N_q}} \sum_{\mathbf{q}} (\phi_{\mathbf{q}}^\dagger + \phi_{-\mathbf{q}}), \quad (14c)$$

Here, a QCP may be present both for a metallic ($r = 0$) and a semimetallic ($r > 0$) conduction band. Section III B treats a spin-one impurity, focusing on the under-screened $K = 1$ pseudogap model. In each of these cases, we consider W (and where present g) to be held fixed and define the distance from criticality to be $\Delta = (J - J_c)/J_c$.

Even with the addition of a degeneracy-lifting field that couples to S_{imp}^z , the Kondo and Bose-Fermi Kondo Hamiltonians [Eqs. (13) and (14)] exhibit spin-rotation symmetry about the z axis and hence conserve the z component of total spin. This ensures that the eigenstates of $\hat{\rho}_{\text{imp}}$ can be chosen to be the conventional basis states $|m\rangle$ such that $S_{\text{imp}}^z |m\rangle = m |m\rangle$. Then,

$$S_e = - \sum_{m=-S}^S p_m \ln p_m. \quad (15)$$

A. $S_{\text{imp}} = \frac{1}{2}$ Kondo and Bose-Fermi Kondo models

For a spin-1/2 Kondo impurity and in the presence of spin-rotation symmetry about the z axis, the eigenvalues of $\hat{\rho}_{\text{imp}}$ are just the impurity spin-up and spin-down occupation probabilities

$$p_{\pm 1/2} = \frac{1}{2} \pm M_{\text{loc}}, \quad (16)$$

and Eq. (2) reduces to

$$S_e = S_2(\frac{1}{2} + M_{\text{loc}}), \quad (17)$$

where

$$S_2(x) = -x \ln x - (1-x) \ln(1-x) \quad (18)$$

is the binary entropy function. Expanding Eq. (17) for $|M_{\text{loc}}| \ll \frac{1}{2}$ gives

$$S_e \simeq \ln 2 - 2M_{\text{loc}}^2 - (4/3)M_{\text{loc}}^4, \quad (19)$$

a result that holds for any $S = \frac{1}{2}$ Kondo model, irrespective of the number and dispersion of the conduction bands.

Equation (19) implies that even in the presence of an infinitesimal magnetic field, the entanglement entropy

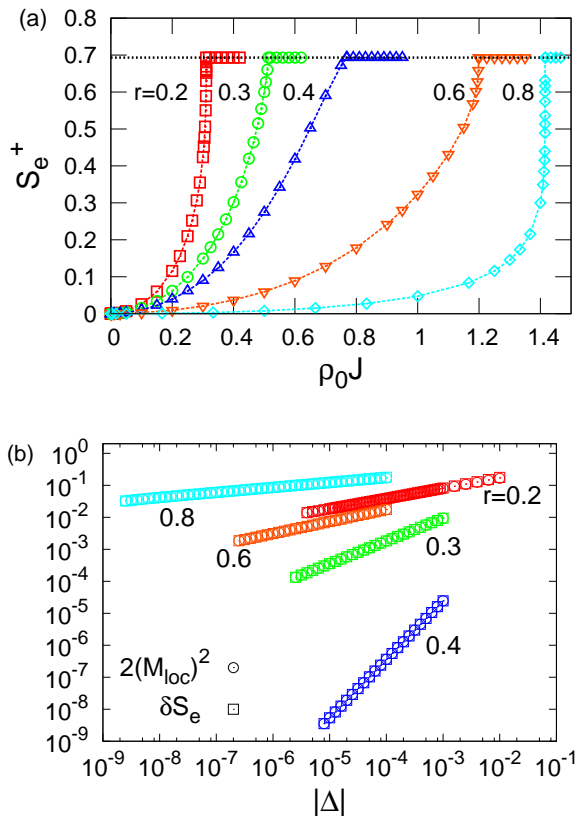


FIG. 3. (Color online) Entanglement entropy in the one-channel, $S_{\text{imp}} = \frac{1}{2}$ pseudogap Kondo model for various combinations of the band exponent r and the dimensionless potential scattering $\rho_0 W$. (a) Degeneracy-lifted entanglement entropy S_e^+ vs dimensionless Kondo coupling $\rho_0 J$. Results for $r = 0.2$ and $r = 0.3$ are at particle-hole symmetry ($W = 0$). Particle-hole-asymmetric results are shown for $r = 0.4$ ($\rho_0 W = 0.109$), $r = 0.6$ ($\rho_0 W = 0.54$), and $r = 0.8$ ($\rho_0 W = 6.2$, plotting $\rho_0 J/6$ on the horizontal axis). In each case, S_e^+ takes its maximum value of $\ln 2 \simeq 0.693$ for all $J \geq J_c$. (b) Spontaneous-symmetry-breaking part of the entanglement entropy $\delta S_e(\Delta)$ and order-parameter M_{loc} (plotted as $2M_{\text{loc}}^2$) vs distance $|\Delta| = (J_c - J)/J_c$ from the QCP in the local-moment phase for several of the cases shown in (a). The coincidence of the two data sets for each r confirms Eq. (20) and straight-line fits yield exponents listed in Table I.

takes its maximum possible value of $\ln 2$ at any magnetic QCP and throughout the Kondo phase. This is true both when the impurity moment is exactly screened with Fermi-liquid excitations (as is the case for $K = 1$) and when it is over-screened with a non-Fermi liquid many-body spectrum (as for $K \geq 2$). Taking into account also Eq. (8), one finds that on approach to the QCP from the local-moment side ($\Delta \rightarrow 0^-$),

$$\delta S_e(\Delta) \simeq 2M_{\text{loc}}^2 \propto (-\Delta)^{2\beta}, \quad (20)$$

realizing Eq. (10) with $a = 2$ as well as exemplifying Eqs. (11a) and (12a).

Another important conclusion that can be drawn from Eqs. (2) and (16) is that S_e^+ vanishes only for $|M_{\text{loc}}| \rightarrow \frac{1}{2}$,

corresponding to a vanishing Kondo coupling J . Even though the Kondo effect is destroyed for $0 < J < J_c$ and the impurity contributes $\ln 2$ to the zero-temperature entropy, the impurity remains entangled with its environment and the ground state cannot be represented in direct-product form.

We supplement these general theoretical considerations with NRG results for several specific cases. For $S_{\text{imp}} = \frac{1}{2}$, we only need to compute $M_{\text{loc}} = -\lim_{T \rightarrow 0} \langle S_{\text{imp}}^z \rangle$, from which S_e can be obtained exactly via Eq. (17). Figure 3(a) shows the degeneracy-lifted entanglement entropy S_e^+ vs $\rho_0 J$ for the one-channel pseudogap Kondo model. This model is known [12] to have (1) a particle-hole-symmetric Kondo-destruction QCP at $J = J_{c,s}(r)$, $W = 0$ for any band exponent r on the range $0 < r < \frac{1}{2}$, and (2) a pair of particle-hole-asymmetric QCPs at $J = J_{c,a}(r)$, $W = \pm W_c(r)$ for any r satisfying $r^* \simeq 3/8 < r < 1$. The figure shows, both for the symmetric case $W = 0$ (illustrated for $r = 0.2$ and 0.3) and the asymmetric one $W \neq 0$ (represented by data for $r = 0.4, 0.6$, and 0.8), that S_e^+ rises from 0 at $J = 0$ to $\ln 2$ at $J = J_c$, and remains pinned at $\ln 2$ throughout the Kondo phase.

Figure 3(b) is a log-log plot of $2M_{\text{loc}}^2$ and δS_e vs $|\Delta|$ in the local-moment phase. Fitting to the power-law forms of Eqs. 8 and (11a) yields the exponents β and β_e listed in Table I. The values of β , along with ones of $1/\delta$ also listed, improve the accuracy of those published previously [13]. For $r = 0.3, 0.4$, and 0.6 , the scaling Eq. (12a) is obeyed to within the (small) estimated nonsystematic error of the exponents. For $r = 0.2, W = 0$ and for $r = 0.8, W \neq 0$ we find minor deviations from scaling (at the 0.5% and 1.5% levels, respectively). In these cases, the exponent $1/\delta$ takes small values that make it very difficult to reach values of $|M_{\text{loc}}| \ll \frac{1}{2}$ and $\delta S_e \ll \ln 2$ even at $J = J_c$ when using the smallest magnetic fields that we can apply numerically (of order $h_{\text{loc}} = 10^{-36} D$ for quadruple-precision floating-point arithmetic). This forces estimation of β and β_e at J values further from J_c where the asymptotic power-law form is obeyed less well.

For most values of r the entanglement exponent satisfies $\beta_e < 1$, meaning that $dS_e^+/d\Delta$ diverges on approach to the QCP from the local-moment side. However, for $0.35 \lesssim r < \frac{1}{2}$ at particle-hole symmetry, as well as for $0.35 \lesssim r \lesssim 0.45$ away from this symmetry (exemplified in Table I by $r = 0.4$, $\rho_0 W = 0.109$), one instead finds $\beta_e > 1$, leading to a much weaker feature in S_e^+ vs Δ at the location of the quantum phase transition.

We have also performed NRG calculations for the two-channel pseudogap Kondo model [the case of Eq. (13) with $K = 2$], which is predicted [12, 15, 37] for $0 < r < r_{\text{max}}$ (where $0.23 < r_{\text{max}} < 0.24$) to have a particle-hole-symmetric QCP between a local-moment phase and a non-Fermi liquid overscreened-Kondo phase. Equation (20) is predicted to hold independent of K , and indeed our numerical results summarized in Table II support this picture: any differences between the cases $K = 1$ and $K = 2$ arise just from the two models having their

r	$\rho_0 W$	β	$1/\delta$	β_e
0.2	0	0.16025(1)	0.02645(4)	0.324(2)
0.3	0	0.35499(2)	0.07398(2)	0.71007(4)
0.4	0.109	0.57553(2)	0.15606(3)	1.15106(2)
0.6	0.54	0.18759(2)	0.11696(5)	0.3754(3)
0.8	6.2	0.07578(2)	0.06373(3)	0.156(2)

TABLE I. Exponents β , δ , and β_e defined in Eqs. (8), (9), and (11a), respectively, for the $S_{\text{imp}} = \frac{1}{2}$, one-channel Kondo model with the five combinations of the band exponent r and dimensionless potential scattering $\rho_0 W$ illustrated in Fig. 3. Parentheses enclose the estimated nonsystematic error in the last digit. The exponents obey Eq. (12a) within the errors, apart from weak violations for $r = 0.2$ and $r = 0.8$, where the small values of $1/\delta$ impede accurate evaluation of β and β_e .

r	β	$1/\delta$	β_e
0.05	0.050(1)	0.001815(2)	0.140(5)
0.1	0.150(2)	0.013075(2)	0.327(4)
0.15	0.330(1)	0.036233(8)	0.667(3)
0.2	0.908(3)	0.09205(2)	1.815(9)

TABLE II. Exponents β , $1/\delta$, and β_e defined in Eqs. (8), (9), and (11a), respectively, for the $S_{\text{imp}} = \frac{1}{2}$, two-channel Kondo model at particle-symmetry ($W = 0$) and four different values of the band exponent r . Parentheses enclose the estimated nonsystematic error in the last digit. The exponents obey Eq. (12a) to within a margin that is within nonsystematic errors for $r = 0.2$, but becomes larger for lower values of r , likely due to the small values of exponent $1/\delta$.

own order-parameter exponents $\beta(r)$.

The final $S_{\text{imp}} = \frac{1}{2}$ model that we have studied numerically is the Ising-symmetry Bose-Fermi Kondo model [Eq. (14)]. As exemplified in Fig. 2 for the case of conduction-band exponent $r = 0$ and a sub-Ohmic bosonic-bath exponent $s = 0.8$, NRG calculations once again confirm that δS_e obeys Eq. (20) on approach to the Kondo-destruction QCP from the local-moment side ($\Delta < 0$), whereas in the Kondo-screened phase ($\Delta > 0$) we find $S_e(\Delta, 0) = \ln 2$. Just as in pure-fermionic Kondo models, S_e^+ rises on approach to phase boundary from the local-moment side to attain its maximum possible value at the QCP and throughout the Kondo phase.

The behavior of the entanglement entropy in the Bose-Fermi Kondo model is in marked contrast with that of the sub-Ohmic spin-boson model, described by Eq. (5) with

$$H_{\text{host}} = \sum_{\mathbf{q}} \omega_{\mathbf{q}} \phi_{\mathbf{q}}^{\dagger} \phi_{\mathbf{q}}, \quad (21a)$$

$$H_{\text{imp}} = h_{\text{loc}} S_{\text{imp}}^z - \Delta_x S_{\text{imp}}^x \quad (21b)$$

$$H_{\text{host-imp}} = g S_{\text{imp}}^z \sum_{\mathbf{q}} (\phi_{\mathbf{q}}^{\dagger} + \phi_{-\mathbf{q}}), \quad (21c)$$

where the dispersion $\omega_{\mathbf{q}}$ satisfies Eq. (7) with $0 < s < 1$. NRG studies [7, 8] show that S_e rises on approach to the QCP from *either* phase, and exhibits a cusp peak at a non-universal value that falls short of the maximum pos-

sible value $\ln 2$. This departure from the entanglement found in the Bose-Fermi Kondo model seems surprising, given that both models map [38, 39] to a classical Ising model with long-range ferromagnetic interactions that decay for large separations d as $1/d^{1+s}$ where s is the bosonic bath exponent. The two quantum-mechanical models are thought to share the same critical exponents [20, 23, 24], at least for $\frac{1}{2} < s < 1$.

However, the classical mapping and the resulting critical exponents describing the response to a local magnetic field along the z axis take no account of the different global symmetries of the two models. The Kondo model exhibits a global $U(1)$ spin symmetry leading to a conserved total spin z component, as well as an emergent $SU(2)$ spin symmetry at the Kondo-screened fixed point. By contrast, the spin-boson model exhibits no spin symmetry at the Hamiltonian level (at least in non-trivial cases where Δ_x and g are both nonzero), while the two stable fixed points exhibit emergent $U(1)$ symmetries leading to conservation of total spin x at the delocalized fixed point (analogous to the Kondo phase) and conservation of total spin z at the localized (local-moment) fixed point.

In the absence of a globally conserved total spin z component we cannot assume that the eigenstates of the impurity reduced density operator are also eigenstates of S_{imp}^z . Instead, the properties $\text{Tr} \hat{\rho}_{\text{imp}} = 1$ and $\text{Tr}(\hat{\rho}_{\text{imp}} \boldsymbol{\sigma}) = 2\langle \mathbf{S} \rangle$ are sufficient to fully specify the impurity reduced density operator as

$$\hat{\rho}_{\text{imp}} = \frac{1}{2} I + \langle \mathbf{S}_{\text{imp}} \rangle \cdot \boldsymbol{\sigma}, \quad (22)$$

where I is the 2×2 identity operator. Then the entanglement entropy is given exactly by Eq. (2) with two eigenvalues [8]

$$p_{\pm} = \frac{1}{2} \pm \sqrt{\langle S_{\text{imp}}^x \rangle^2 + \langle S_{\text{imp}}^y \rangle^2 + \langle S_{\text{imp}}^z \rangle^2}. \quad (23)$$

Clearly, S_e attains its maximum possible value of $\ln 2$ if and only if $\langle \mathbf{S}_{\text{imp}} \rangle = \mathbf{0}$, a condition that is satisfied throughout the Kondo phase of the Bose-Fermi Kondo model and also at the QCP. By contrast, the nonzero value of Δ_x necessary to produce a quantum phase transition in the sub-Ohmic spin-boson model leads to a nonzero $\langle S_{\text{imp}}^x \rangle$ in both phases. We expect that for fixed g , $S_e(h_{\text{loc}} = 0)$ decreases smoothly from $\ln 2$ as Δ_x increases from zero, and $S_e(h_{\text{loc}} = 0)$ shows no feature at the QCP. The addition of an infinitesimal field along the z axis creates a nonzero $\langle S_{\text{imp}}^z \rangle$ only in the delocalized phase, thereby yielding [40] a correction δS_e obeying Eqs. (10), (11a), and (12a), and leading S_e^+ to exhibit a cusp peak in all cases where $2\beta < 1$. We speculate that similar behavior would arise in the Ising-symmetry Bose-Fermi Kondo model in the presence of a transverse local field [41], although we have not explicitly tested this conjecture.

B. $S_{\text{imp}} = 1$ single-channel pseudogap Kondo model

For a spin-1 Kondo impurity and in the presence of spin-rotation symmetry about the z axis, the eigenvalues of $\hat{\rho}_{\text{imp}}$ can be parameterized

$$p_{\pm 1} = \frac{1}{2}(n_0 \pm M_{\text{loc}}), \quad (24a)$$

$$p_0 = 1 - n_0, \quad (24b)$$

where we have introduced $n_0 = \langle (S_{\text{imp}}^z)^2 \rangle$. For such an impurity, we focus exclusively on the one-channel pseudogap Kondo model. At particle-hole symmetry ($W = 0$), this model has a QCP for any band exponent r on the range $0 < r < r_{\text{max}}$ where $0.26 < r_{\text{max}} < 0.27$, while for $W \neq 0$ there is a pair of asymmetric QCPs for any $r^* \simeq 0.245 < r < 1$ [12]. Each QCP separates (1) a local-moment phase with a decoupled spin-one impurity degree of freedom and a ground-state moment-squared $\mu^2 = S_{\text{imp}}(S_{\text{imp}} + 1) = 2$ from (2) an under-screened Kondo phase in which the impurity spin and the conduction band form a many-body ground state with a residual moment-squared $\mu^2 = 3(2 + r)/8$ for $W = 0$ or $\mu^2 = 3/4$ for $W \neq 0$.

In the Kondo phase, the system shows an infinitesimal response to an infinitesimal degeneracy-lifting field, and we can take the eigenvalues of $\hat{\rho}_{\text{imp}}$ to be $p_{\pm 1} = p_0 = 1/3$, which corresponds to $M_{\text{loc}} = 0$, $n_0 = 2/3$, and $S_e(\Delta, 0) = \ln 3$. Interestingly, even though the spin-1 impurity is only partially screened, the entanglement entropy still takes its maximal value of $\ln(2S_{\text{imp}} + 1)$.

In the local-moment phase, by contrast, the ground state exhibits spontaneously broken $SU(2)$ symmetry, and it is natural that n_0 should rise above $2/3$. However, it is plausible (and we confirm below) that close to the QCP, deviations of n_0 from $2/3$ will be smaller than those of the order parameter M_{loc} from zero, and that the former can safely be neglected. More specifically, one can conjecture that

$$n_0(h_{\text{loc}} = 0^+) - 2/3 \propto (-\Delta)^{\beta_n}, \quad (25)$$

with $\beta_n > \beta$. Substituting Eqs. (24) into Eq. (2), setting $n_0 = 2/3$ and keeping only leading terms in M_{loc} , one arrives at the result

$$\delta S_e(\Delta) \approx \frac{3}{4} M_{\text{loc}}^2 \propto (-\Delta)^{2\beta}, \quad (26)$$

providing a realization of Eq. (10) with $a = 3/4$. As was the case for $S_{\text{imp}} = \frac{1}{2}$, the predicted behavior is consistent with Eqs. (11a) and (12a).

Figure 4 presents NRG results for three combinations of the pseudogap exponent and the dimensionless potential scattering: $(r, \rho_0 W) = (0.25, 0)$, $(0.4, 0.5)$, and $(0.6, 0.8)$. Here, we have computed $M_{\text{loc}} = -\langle S_{\text{imp}}^z \rangle$ and $n_0 = \langle (S_{\text{imp}}^z)^2 \rangle$, then used Eqs. (2) and (24) to find S_e . Figure 4(a) shows that on approach to each QCP from the local-moment side, M_{loc} , $n_0 - 2/3$, and δS_e vanish in power-law fashion according to Eqs. (8), (25), and (11a),

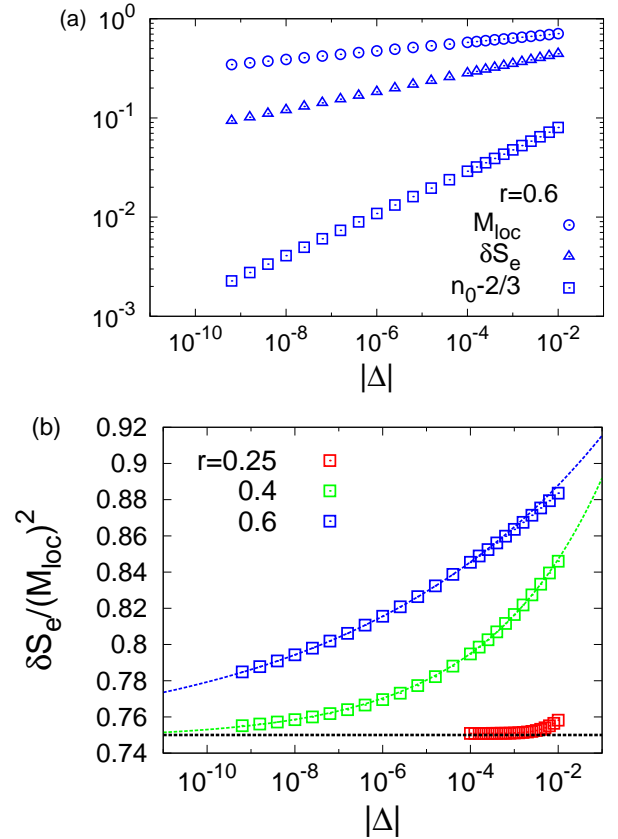


FIG. 4. (Color online) Approach from the local-moment side to the quantum critical point of the one-channel, $S_{\text{imp}} = 1$ pseudogap Kondo model for three combinations of the pseudogap exponent and the dimensionless potential scattering: $(r, \rho_0 W) = (0.25, 0)$, $(0.4, 0.5)$, and $(0.6, 0.8)$. (a) Log-log plot of M_{loc} , $n_0 - 2/3$, and δS_e vs $|\Delta|$ for $r = 0.6$, with the linear variations exemplifying Eqs. (8), (25), and (11a), respectively. (b) Ratio $\delta S_e / M_{\text{loc}}^2$ vs $|\Delta|$. The convergence of the ratio to 0.75 as $\Delta \rightarrow 0^-$ (albeit at a rate that decreases with increasing r) confirms the validity of Eq. (26).

respectively. The exponents extracted from plots such as this are summarized in Table III for the three examples shown in the figure, plus the particle-hole-symmetric QCPs for $r = 0.1, 0.15$, and 0.2 . In each case, the exponents satisfy $\beta_n > 3\beta$, confirming the conjecture that deviations of n_0 from $2/3$ can be neglected in the vicinity of the QCP. Equation (12a) is also satisfied with one minor violation (for $r = 0.25$) and one more significant one for $r = 0.6$ that can be attributed to the same cause (a small exponent $1/\delta$) as in the one-channel $S_{\text{imp}} = \frac{1}{2}$ Kondo model.

Figure 4(b) plots the ratio $\delta S_e / M_{\text{loc}}^2$ on the same logarithmic $|\Delta|$ scale as used for Figure 4(a). For $r = 0.25$, $W = 0$, the ratio converges rapidly to 0.75, as predicted in Eq. (26). The convergence is rather slower for $r = 0.4$, $\rho_0 W = 0.5$, and markedly slower for $r = 0.6$, $\rho_0 W = 0.8$. This trend can be explained by the taking into account the leading correction to Eq. (26) in

r	$\rho_0 W$	β	β_n	β_e
0.1	0	0.062(5)	0.19(1)	0.13(1)
0.15	0	0.116(1)	0.386(5)	0.24(1)
0.2	0	0.207(1)	0.787(4)	0.423(4)
0.25	0	0.51(1)	2.7(1)	1.00(5)
0.4	0.5	0.08960(5)	0.4509(3)	0.180(1)
0.6	0.8	0.04300(5)	0.2128(2)	0.089(1)

TABLE III. Exponents β , β_n , and β_e defined in Eqs. (8), (25), and (11a), respectively, for the $S_{\text{imp}} = 1$, one-channel Kondo model six combinations of the band exponent r and the dimensionless potential scattering $\rho_0 W$. Parentheses enclose the estimated nonsystematic error in the last digit. In each case, $\beta_n \geq 3\beta$, implying that variations of n_0 are negligible compared to those of M_{loc} in the vicinity of the quantum critical point. The exponents obey Eq. (12a) within the errors, apart from a weak violation for $r = 0.2$ and a stronger one for $r = 0.6$, where the small value $1/\delta = 0.02589(2)$ impedes accurate evaluation of β and β_e .

situations where $\beta_n > 2\beta$, namely,

$$\delta S_e(\Delta) \approx \frac{3}{4} M_{\text{loc}}^2 + \frac{9}{32} M_{\text{loc}}^4, \quad (27)$$

and noting in Table III the decrease in the value of β as r increases toward 1. We can extrapolate the ratio $\delta S_e/M_{\text{loc}}^2$ for $\Delta \rightarrow 0$ to obtain 0.7499(3) and 0.746(6) for $r = 0.4$ and $r = 0.6$, respectively, in excellent agreement with the predicted value $a = 3/4$. We therefore take Figure 4(b) as providing confirmation of the relation Eq. (26).

IV. ANDERSON MODELS

In this section we consider non-degenerate Anderson impurity models characterized by an impurity Hamiltonian

$$H_{\text{imp}} = \epsilon_d n_d + U n_{d\uparrow} n_{d\downarrow} + h_{\text{loc}} (n_{d\uparrow} - n_{d\downarrow})/2, \quad (28)$$

where d_σ destroys an electron of energy ϵ_d and spin z component σ electron at the impurity site, $n_{d\sigma} = d_\sigma^\dagger d_\sigma$ and $n_d = n_{d\uparrow} + n_{d\downarrow}$ are impurity number operators, and U is the on-site Coulomb interaction. Such models differ from their Kondo counterparts by allowing charge fluctuations on the impurity site. We will show that such fluctuations can significantly modify the behavior of the entanglement entropy in the vicinity of the continuous quantum phase transition between Kondo-screened and local-moment (Kondo-destroyed) phases. In particular, in the presence of an infinitesimal symmetry-breaking field, the entanglement entropy in general neither exhibits a peak at the QCP (as it does in the sub-Ohmic spin-boson model) nor attains its maximum possible value at the QCP and throughout the Kondo phase (as is the case in the Kondo and Bose-Fermi Kondo models discussed in Sec. III).

Under conditions of spin-rotation symmetry about the z axis, the eigenstates of the impurity reduced density operator can be taken [43] to be the conventional basis states $|0\rangle$, $|\sigma\rangle = d_\sigma^\dagger |0\rangle$, and $|2\rangle = d_\uparrow^\dagger d_\downarrow^\dagger |0\rangle$, with eigenvalues that can be written as

$$p_2 = \langle n_{d\uparrow} n_{d\downarrow} \rangle, \quad (29a)$$

$$p_\uparrow = f/2 + M_{\text{loc}}, \quad (29b)$$

$$p_\downarrow = f/2 - M_{\text{loc}}, \quad (29c)$$

$$p_0 = 1 - f - p_2, \quad (29d)$$

in terms of the local-moment fraction (i.e., single-occupation probability) $f = \langle n_d \rangle - 2p_2$ and the local moment $M_{\text{loc}} = \langle \frac{1}{2}(n_{d\uparrow} - n_{d\downarrow}) \rangle$, such that $0 \leq f \leq 1$ and $|M_{\text{loc}}| \leq f/2$. Then Eq. (2) can be written

$$S_e = f S_2 \left(\frac{1}{2} + \frac{M_{\text{loc}}}{f} \right) + (1-f) S_2 \left(\frac{p_2}{1-f} \right), \quad (30)$$

which can be interpreted as the sum of a binary spin entanglement entropy with weight f and a binary charge entanglement entropy with weight $(1-f)$. The parallel between the spin and charge parts of S_e can be made clearer by defining a ‘‘local charge’’ $Q_{\text{loc}} = p_2 - p_0$, satisfying $|Q_{\text{loc}}| \leq 1 - f$, so that

$$\frac{p_2}{1-f} = \frac{1}{2} + \frac{Q_{\text{loc}}}{2(1-f)}. \quad (31)$$

In the absence of a symmetry-breaking field h_{loc} , we can set $M_{\text{loc}} = 0$ in Eqs. (29), and use Eq. (2) to obtain

$$S_e(h_{\text{loc}} = 0) = -(1-f-p_2) \ln(1-f-p_2) - f \ln(f/2) - p_2 \ln p_2. \quad (32)$$

Since f and p_2 are nontrivial functions of U , ϵ_d , and Γ , it is clear that Eq. (32) can encompass much richer behavior than the corresponding Kondo-model result $S_e(h_{\text{loc}} = 0) = \ln 2$. Differentiating Eq. (32) with respect to p_2 for a fixed local-moment fraction f yields

$$\left(\frac{\partial S_e}{\partial p_2} \right)_f = \ln \frac{p_0}{p_2}, \quad (33)$$

which implies that for a given value of f , $S_e(h_{\text{loc}} = 0)$ is greatest for equal occupation of the impurity configurations $|0\rangle$ and $|2\rangle$ (i.e., $Q_{\text{loc}} = 0$), and is smallest when one or other of the configurations is ruled out.

In the local-moment phase near the boundary with the Kondo phase, we expect an infinitesimal field $h_{\text{loc}} = 0^+$ to establish a local magnetization $|M_{\text{loc}}| \ll \frac{1}{2}$ with negligible shift of f and p_2 . Under these circumstances, an expansion of S_e in powers of M_{loc} shows the spontaneous-symmetry-breaking part of the entanglement entropy to be

$$\delta S_e(\Delta) \simeq 2M_{\text{loc}}^2/f \propto (-\Delta)^{2\beta}, \quad (34)$$

providing yet another realization of Eqs. (10), (11a), and (12a), this time with $a = 2/f$. Since the local-moment

fraction satisfies $0 \leq f \leq 1$, the critical part of the entanglement in nondegenerate Anderson models is generally enhanced by a factor of $1/f$ compared to its counterpart in $S_{\text{imp}} = \frac{1}{2}$ Kondo models [see Eq. (20)].

For the purposes of numerical study, we focus on the one-channel Anderson impurity model described by the Hamiltonian in Eq. (5) with H_{host} as given in Eq. (13a), H_{imp} as in Eq. (28) and

$$H_{\text{host-imp}} = \frac{V}{\sqrt{N_k}} \sum_{\mathbf{k}, \sigma} (c_{\mathbf{k}\sigma}^\dagger d_\sigma + \text{H.c.}), \quad (35)$$

The hybridization matrix element V between the impurity site and the conduction band is conventionally re-expressed in terms of the hybridization width $\Gamma = \pi \rho_0 V^2$. We have computed $\langle n_{d,\sigma} \rangle$ and $\langle n_{d,\uparrow} n_{d,\downarrow} \rangle$, then used Eqs. (2) and (29) to find S_e .

In the following we take U and ϵ_d to be fixed, either at particle-hole symmetry ($\epsilon_d = -U/2$) or away from it ($\epsilon_d \neq -U/2$). We then find the location of the QCP at a critical hybridization width $\Gamma_c(U, \epsilon_d)$, and thereafter define the distance from criticality as $\Delta = (\Gamma - \Gamma_c)/\Gamma_c$. The critical responses to a local magnetic field near the symmetric and asymmetric QCPs of the pseudogap Anderson model belong in the same universality classes as the respective QCPs of the $S_{\text{imp}} = \frac{1}{2}$ Kondo model [12–14, 16, 17].

In the subsections that follow, we first consider two special cases ($U = -2\epsilon_d$ and $U = \infty$) in which $S_e(h_{\text{loc}} = 0)$ in Eq. (32) reduces to a function of one variable, the local-moment fraction, thereby simplifying analysis of the behavior of the entanglement entropy in the vicinity of the QCP. Afterward, we present illustrative examples of the entanglement properties for more general cases.

A. Particle-hole symmetry: $U = -2\epsilon_d$

For the particle-hole-symmetric case $\epsilon_d = -U/2$, we have $\langle n_d \rangle = 1$ and $p_0 = p_2 = (1 - f)/2$. As a result, Eq. (32) reduces to

$$S_e(h_{\text{loc}} = 0) = S_2(f) + \ln 2, \quad (36)$$

which increases monotonically from $\ln 2$ to $\ln 4$ as $|f - \frac{1}{2}|$ decreases from $\frac{1}{2}$ to 0. Equation (33) tells us that for a given value of f , $S_e(h_{\text{loc}} = 0)$ is greater for this symmetric case than for any value $\epsilon_d \neq -U/2$ that leads to $p_0 \neq p_2$.

In the conventional situation of on-site Coulomb repulsion (i.e., $U > 0$), there is a monotonic evolution of the local-moment fraction from $f = 1$ at $\Gamma = 0$ to $f \rightarrow \frac{1}{2}$ for $\Gamma \gg U$, reflecting the increased admixture of the $n_d = 0, 2$ excited configurations into the $n_d = 1$ ground state of the isolated impurity. This behavior, which is exemplified in Fig. 5(a) for $r = 0.4$ and two cases, $U/D = 0.005$ and 0.5, leads to a monotonic increase in $S_e(h_{\text{loc}} = 0)$ from $\ln 2$ at $\Gamma = 0$ to $\ln 4$ for $\Gamma \gg U$. Both f and $S_e(h_{\text{loc}} = 0)$ increase in a smooth, featureless

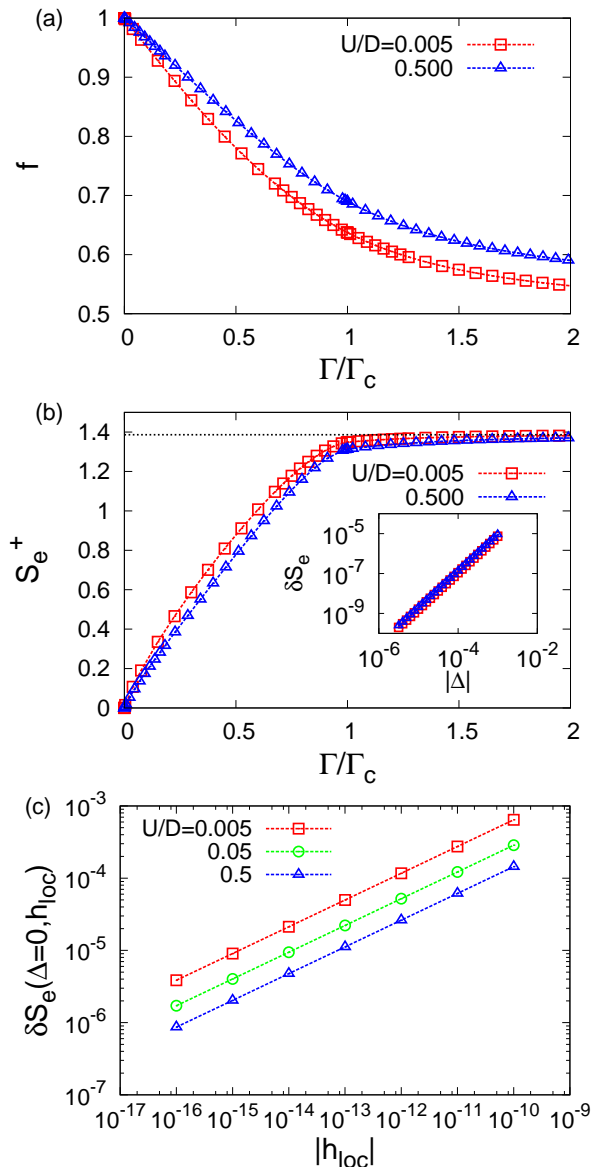


FIG. 5. (Color online) Particle-hole-symmetric pseudogap Anderson model with band exponent $r = 0.4$ for different values of U/D : (a) Local-moment fraction f and (b) symmetry-lifted entanglement entropy S_e^+ , both vs hybridization width Γ scaled by its critical value Γ_c . In the limit of large Γ , S_e^+ approaches its maximum value of $\ln 4 \approx 1.386$. Inset to (b): Spontaneous-symmetry-breaking part of the entanglement entropy δS_e vs $|\Delta|$ [where $\Delta = (\Gamma - \Gamma_c)/\Gamma_c$] for the two cases shown in (a) and (b). The linear variations of the points on this log-log plot are consistent with Eq. (11a) with $\beta_e = 1.8288(1)$. (c) Local-field-dependent part of the entanglement entropy δS_e vs h_{loc} at the critical hybridization width, showing behavior consistent with Eq. (11b) with $1/\delta_e = 0.3703(1)$.

fashion as Γ rises through Γ_c . [The mapping $U \rightarrow -U$, $\epsilon_d \rightarrow -\epsilon_d$, $\Gamma \rightarrow \Gamma$ takes one to an Anderson model with on-site attraction, which for a pseudogap density of states

features quantum phase transitions between local-charge and charge-Kondo phases [42]. Since the mapping transforms $f \rightarrow 1 - f$, it preserves $S_e(h_{\text{loc}} = 0)$. We will not consider cases $U < 0$ any further in this paper.]

We have already argued that the effect of a local magnetic field $h_{\text{loc}} = 0^+$ is to reduce the entanglement entropy by an amount that varies near the QCP according to Eq. (34). Since the QCP always occurs at a local moment fraction $f > \frac{1}{2}$, $S_e(h_{\text{loc}} = 0)$ has a positive slope at $\Gamma = \Gamma_c$. It is therefore the case that the degeneracy-lifted entanglement entropy has a positive slope on both sides of the quantum phase transition. In other words, it is impossible for S_e^+ to exhibit a peak at the QCP. In cases where the order-parameter exponent satisfies $\beta < 1$, we expect a divergence of $dS_e^+/d\Gamma$ on approach to the QCP from the local-moment side. By contrast, for $2\beta > 1$, the spontaneous-symmetry-breaking part of the entanglement entropy should vanish faster than the linear variation $S_e(h_{\text{loc}} = 0)$ and S_e^+ should therefore be essentially featureless on passing through the quantum phase transition.

Figure 5(b) plots S_e^+ over a broad range $0 \leq \Gamma/\Gamma_c \leq 2$ for $r = 0.4$, a case [13, 44] where $\beta = 0.91440(2) > \frac{1}{2}$. The curves for different values of U are quantitatively different, but share the same principal features: a smooth rise of S_e^+ from zero in the decoupled-impurity limit $\Gamma/U \rightarrow 0$, with a linear variation through $\Gamma = \Gamma_c$ [not shown in detail in Figure 5(b)] leading to a saturation $S_e^+ \rightarrow \ln 4$ in the uncorrelated limit $\Gamma/U \rightarrow \infty$.

We find that for a given value of Δ , S_e^+ in the particle-hole-symmetric Anderson model generically exceeds S_e^+ in the counterpart $S_{\text{imp}} = \frac{1}{2}$ Kondo model with the same band exponent r . This is a natural consequence of the Anderson impurity being entangled with both the spin and charge degrees of freedom of its environment. In the limit $U/D \rightarrow \infty$, however, the form of $S_e^+(\Delta)$ for the Anderson model converges to the corresponding function for the Kondo model. [The Kondo function $S_e^+(\Delta)$ for several values of r can be extracted from Fig. 3(a) by rescaling the horizontal axis from $\rho_0 J$ to $\Delta = (J - J_c)/J_c$.] Conversely, as U/D approaches zero, the critical hybridization vanishes [45] as $\Gamma_c/D \propto (U/D)^{1-r}$ while S_e^+ becomes ever closer to $\ln 4$ throughout the region $\Gamma \geq \Gamma_c$; a trend that smoothly merges into the physics of a non-interacting resonant level ($U = \epsilon_d = 0$) where $S_e^+ = \ln 4$ for any $\Gamma > 0$.

Examination of the spontaneous-symmetry-breaking part of the entanglement entropy allows quantitative testing of Eq. (34). The inset to Fig. 5(b) illustrates log-log plots of $\delta S_e(\Delta)$ that for $U/D = 0.5$ and 0.005 can be fitted to Eq. (11a) with $\beta_e = 1.8288(1)$, matching within estimated error the scaling prediction of Eq. (12a) using the aforementioned value $\beta = 0.91440(2)$. Table IV shows that the ratio $\delta S_e/M_{\text{loc}}^2$ is captured to high accuracy by Eq. (34).

We conclude our discussion of the particle-hole symmetric Anderson model by presenting results for the effect of a finite local magnetic field. Figure 5(c) plots the

U/D	f_c	$2/f_c$	b
0.005	0.637220	3.13863	3.1386(1)
0.05	0.646976	3.09131	3.0913(2)
0.5	0.689800	2.89939	2.8994(1)

TABLE IV. Properties at the quantum critical point of the particle-hole-symmetric pseudogap Anderson model for $r = 0.4$ and three values of U/D : local-moment fraction f_c (from NRG), and the predicted and actual values of $\delta S_e/M_{\text{loc}}^2$ in a field $h_{\text{loc}} = 0^+$, i.e., $2/f_c$ based on Eq. (34) and the ratio b computed directly from NRG values of δS_e and M_{loc} .

local-field-dependent part of the entanglement entropy $\delta S_e(\Delta, h_{\text{loc}})$ as a function of h_{loc} for fixed $\Delta = 0$ (i.e., at the critical hybridization width). The linear variation of the data for three different values of U/D fulfills the prediction of Eq. (11b), while the fitting of quadruple-precision results spanning fields down to $h_{\text{loc}} = 10^{-25}D$ (data not shown) yields an exponent $1/\delta_e = 0.37032(2)$ in excellent agreement with the value $0.37032(4)$ deduced from Eq. (12b) using the previously known value $1/\delta = 0.18516(2)$.

B. Maximal particle-hole asymmetry: $U = \infty$

For the case $U = \infty$ of maximal particle-hole asymmetry, the parameters entering Eq. (32) reduce to $p_2 = 0$, $f = \langle n_d \rangle$, and $p_0 = 1 - f$, so that

$$S_e(h_{\text{loc}} = 0) = S_2(f) + f \ln 2. \quad (37)$$

For a given f , this value is smaller by $(1 - f) \ln 2$ than its counterpart for the symmetric model; indeed, Eq. (33) indicates that for fixed f , $S_e(h_{\text{loc}} = 0)$ takes its smallest value when $U = \infty$ (and also when $U = -\infty$, leading to $p_0 = 0$). Under variation of the local-moment fraction, $S_e(h_{\text{loc}} = 0)$ increases from 0 at $f = 0$ to a maximum value of $\ln 3$ at $f = 2/3$, and then decreases to reach $\ln 2$ at $f = 1$.

For given values of r and ϵ_d , a quantum phase transition between local-moment and Kondo phases will occur at some $\Gamma = \Gamma_c$. Unlike the situation at particle-hole symmetry, where $S_e(h_{\text{loc}} = 0)$ varies linearly with Δ near the QCP, the variation for any $\epsilon_d \neq -U/2$ is described by

$$S_e(\Delta, 0) - S_e(0, 0) \simeq A|\Delta|^{1-\tilde{\gamma}} \text{sgn } \Delta, \quad (38)$$

where $\tilde{\gamma}$ is the charge-susceptibility exponent at the QCP and A may be positive or negative. For $U = \infty$, this variation can be deduced by writing

$$dS_e(\Delta, 0)/d\Delta = [dS_e(h_{\text{loc}} = 0)/df] \cdot (df/d\Delta) \quad (39)$$

and noting that while $dS_e(h_{\text{loc}} = 0)/df$ is regular near the QCP, $df/d\Delta = \partial \langle n_d \rangle / \partial \Delta \propto |\Delta|^{-\tilde{\gamma}}$ can be nonanalytic [17, 46]. For $0.55 \lesssim r < 1$, the charge susceptibility exponent $\tilde{\gamma}$ is positive [46], signaling a critical divergence

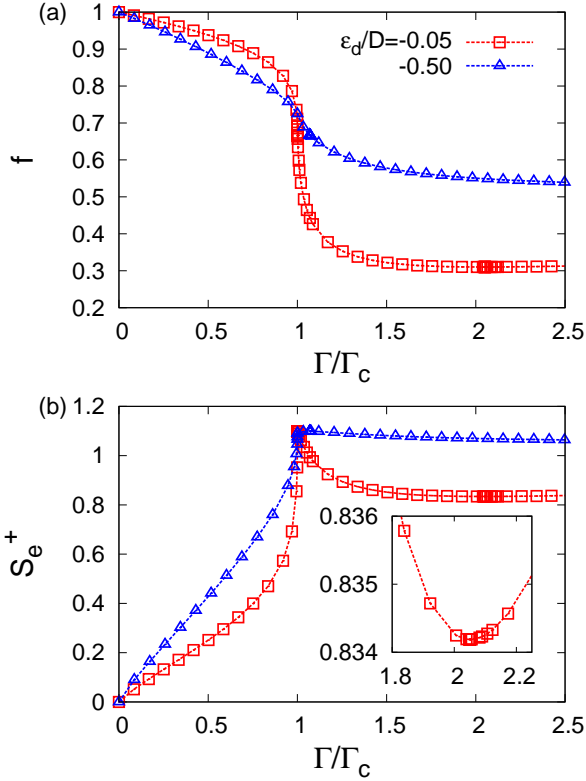


FIG. 6. (Color online) $U = \infty$ pseudogap Anderson model with band exponent $r = 0.6$ for $-\epsilon_d/D = 0.05$ and 0.5 : (a) Local-moment fraction f and (b) degeneracy-lifted entanglement entropy S_e^+ , both vs hybridization width Γ scaled by its critical value Γ_c . For $\epsilon_d = -0.5D$, f decreases monotonically with increasing Γ , and passes through $2/3$ at $\Gamma/\Gamma_c \simeq 1.07$, where S_e^+ peaks at $\ln 3$. For $\epsilon_d = -0.05D$, f drops through $2/3$ (and S_e^+ peaks) at $\Gamma/\Gamma_c \simeq 1.00085$, and f (and S_e^+) reaches a minimum at $\Gamma/\Gamma_c \simeq 2.05$ (Inset). On the wide scale of Γ/Γ_c shown in this figure, the location of the peak in S_e^+ is virtually indistinguishable from the position of the quantum critical point.

of impurity charge fluctuations on approach to the QCP from either phase. The asymmetric QCPs for $r^* \simeq 3/8 \leq r \lesssim 0.55$ instead show a non-divergent charge response, i.e., $\tilde{\gamma} = 0$, a behavior also displayed at the symmetric QCPs that exist for $\epsilon_d = -U/2$ and $0 < r < \frac{1}{2}$.

As a result of the combination of the local-moment contribution from Eq. (34) and the charge contribution from Eq. (38), the degeneracy-lifted entanglement entropy will exhibit a cusp peak at the QCP provided that (1) $dS_e(h_{\text{loc}} = 0)/d\Delta < 0$ at $\Delta = 0$ to ensure that $dS_e^+/d\Delta < 0$ for $\Delta = 0^+$, and (2) $2\beta < 1 - \tilde{\gamma}$ to ensure that $dS_e^+/d\Delta > 0$ for $\Delta = 0^-$. Previous NRG calculations have shown that condition (2) is satisfied at the particle-hole-asymmetric QCPs for $0.42 \lesssim r < 1$ [48]. In what follows, therefore, we focus on whether condition (1) is satisfied.

The sign of $dS_e(h_{\text{loc}} = 0)/d\Delta$ at $\Delta = 0$ can be determined using Eq. (39). From Eq. (37) we see that

$dS_e(h_{\text{loc}} = 0)/df$ is positive for $f < 2/3$ and negative for $f > 2/3$. In the regime $\epsilon_d < 0$ that admits interesting many-body physics, the local-moment fraction has limits $f \rightarrow 1$ for $\Gamma \rightarrow 0$ and $f \rightarrow \frac{1}{2}$ for $\Gamma \rightarrow \infty$ [47]. It might therefore appear plausible that $df/d\Gamma < 0$ and hence $df/d\Delta < 0$ for all intermediate values of Γ . However, NRG calculations show this assumption to be correct only for large values of $|\epsilon_d|/D$. For smaller $|\epsilon_d|/D$, f instead has a minimum at a finite value of Γ , beyond which it increases to approach $\frac{1}{2}$ from below.

We present data here solely for the representative case $r = 0.6$, but have obtained qualitatively similar results for other r values. Figure 6(a) plots f vs Γ/Γ_c for $\epsilon_d/D = -0.05$ and -0.5 . For $\epsilon_d = -0.5D$, f decreases monotonically with increasing hybridization width, passing through $2/3$ at $\Gamma \simeq 1.07\Gamma_c$ where $S_e(h_{\text{loc}} = 0)$ rises to a smooth peak at its maximal value $\ln 3$. For $\epsilon_d = -0.05D$, f drops through $2/3$ and $S_e(h_{\text{loc}} = 0)$ peaks at $\Gamma \simeq 1.00085\Gamma_c$, barely into the Kondo phase. However, in contrast to its behavior for $\epsilon_d = -0.5D$, the local-moment fraction then reaches a minimum value $f \simeq 0.834 \simeq 0.759 \ln 3$ at $\Gamma \simeq 2.05\Gamma_c$ before rising back toward $f = \frac{1}{2}$. Upon further decrease of $|\epsilon_d|/D$ (not shown), the peak in $S_e(h_{\text{loc}} = 0)$ moves ever closer to $\Gamma = \Gamma_c$ and the minimum value of f and a related minimum in $S_e(h_{\text{loc}} = 0)$ become deeper while the location of these minima remains significantly above Γ_c . However, for all $\epsilon_d < 0$ it appears that $dS_e(h_{\text{loc}} = 0)/df > 0$ and $df/d\Delta > 0$ at $\Delta = 0$, meaning that the conditions are never met for the occurrence of a peak in S_e^+ precisely at the QCP.

C. General case

Finally we turn to cases of intermediate particle-hole symmetry, for which no simplification of Eq. (32) is possible. We focus once again on the case $r = 0.6$ representative of the range of band exponents in which $2\beta < 1 - \tilde{\gamma}$, potentially allowing for the occurrence of a peak in S_e^+ at the QCP.

Figure 7 shows results over a wide range of Γ/Γ_c values for $\epsilon_d = -0.05D$ and for $U/D = 0.051, 0.055$, and 0.075 . As U gets closer to $-\epsilon_d$, particle-hole asymmetry grows stronger, as do changes near $\Gamma = \Gamma_c$ in the local-moment fraction [Fig. 7(a)], the double occupancy [Fig. 7(b)], and the degeneracy-lifted entanglement entropy [Fig. 7(c)]. For $U/D = 0.075$ and 0.055 , $S_e(h_{\text{loc}} = 0)$ peaks just inside the local-moment phase at $\Delta \simeq -1.2 \times 10^{-3}$ and -3.2×10^{-4} , respectively. The negative slope of $S_e(h_{\text{loc}} = 0)$ at $\Gamma = \Gamma_c$, combined with the order-parameter exponent satisfying $2\beta < 1 - \tilde{\gamma}$ is sufficient to create a cusp peak in S_e^+ at the QCP. By contrast, for $U/D = 0.051$, $S_e(h_{\text{loc}} = 0)$ peaks just inside the Kondo phase at $\Delta \simeq 5 \times 10^{-5}$, thereby preventing the occurrence of any peak in S_e^+ at $\Delta = 0$ [49]. However, the tiny displacement of the maximum in $S_e(h_{\text{loc}} = 0)$ from $\Delta = 0$ means that in practice it will prove very

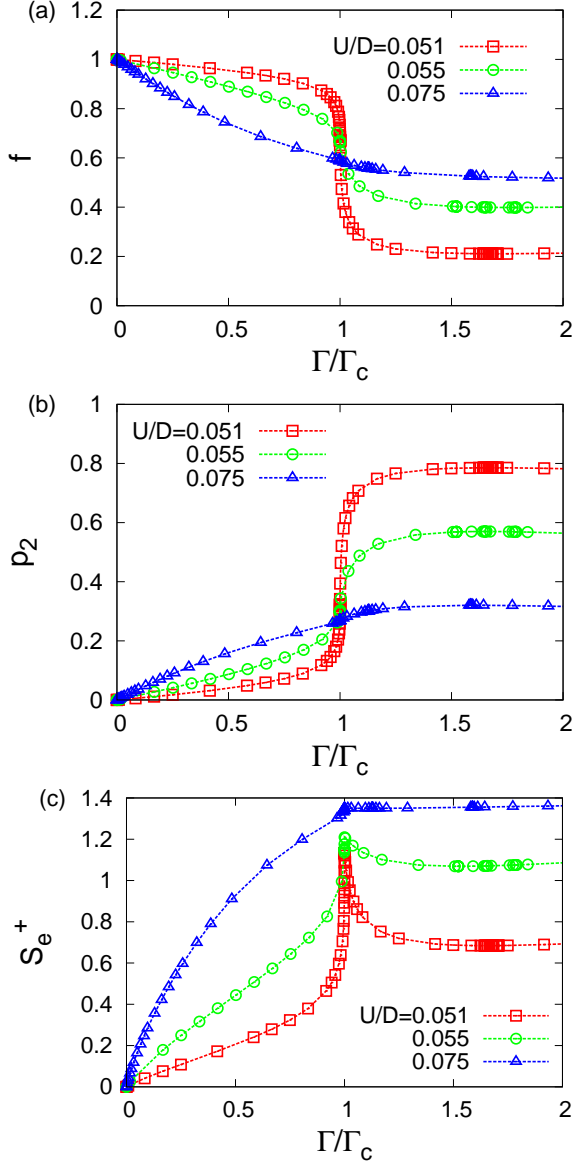


FIG. 7. (Color online) Pseudogap Anderson model with band exponent $r = 0.6$, impurity level energy $\epsilon_d = -0.05D$, and three values of $U \neq -2\epsilon_d$: (a) Local-moment fraction f , (b) double occupancy p_2 , and (c) degeneracy-lifted entanglement entropy S_e^+ vs hybridization width Γ scaled by its critical value Γ_c . A peak in S_e^+ occurs precisely at the quantum critical point for $U/D = 0.075$ and 0.055 , but shifted slightly into the Kondo phase ($\Gamma > \Gamma_c$) for $U = 0.051D$. These cases are indistinguishable on the wide scale of Γ/Γ_c shown in this figure.

hard to distinguish cases where there really is a peak in the degeneracy-lifted entanglement entropy at the QCP from ones where a peak lies close by inside the Kondo phase.

Deeper into the Kondo phase, $S_e^+ \equiv S_e(h_{loc} = 0)$ exhibits a broad minimum, which is centered at $\Gamma/\Gamma_c \simeq 1.65, 1.52,$ and 1.13 for $U/D = 0.051, 0.055,$ and $0.075,$

respectively. The minimum in S_e^+ weakens as U increases toward $-2\epsilon_d$, consistent with the monotonic rise in entanglement entropy throughout the Kondo phase that is seen at particle-hole symmetry [Fig. 5(c)].

The physics near the QCP is shown in more detail in Fig. 8, once again for a representative case $r = 0.6$ and $\epsilon_d = -0.05D$. Figure 8(a) plots the critical part of the entanglement entropy in the absence of a local magnetic field for $U = 0.055D$. The divergent charge susceptibility produces a nonanalytic variation of $S_e(\Delta, 0) - S_e(0, 0)$ that is well-captured by Eq. (38), even though the power-law variation in the local-moment phase is confined to a rather narrow region of $|\Delta|$ values due to the aforementioned peak in $S_e(h_{loc} = 0)$ at $\Delta = -3.2 \times 10^{-4}$. The inferred exponent $\tilde{\gamma} = 0.23(2)$ is fully consistent with the directly-computed [17, 46] charge-susceptibility exponent $\tilde{\gamma} = 0.210(2)$. Figure 8(b) shows the local-magnetic-field response at the QCP ($\Delta = 0$) for $U/D = 0.051, 0.055,$ and 0.075 . Fitting to Eq. (11b) yields an exponent $1/\delta_e = 0.2340(1)$, in excellent agreement with Eq. (12b) given that $2/\delta = 0.23392(8)$ based on Table I.

V. DISCUSSION

One universal feature of our results is the presence of a nonzero entanglement on entry to the local-moment (Kondo-destroyed) phase. Such a residual entanglement implies that the ground state is not a simple product of an impurity state and an environmental state. This result has significant implications for theoretical and numerical descriptions of the Kondo-destroyed phase. For example, within a large- N mean field theory of the pseudogap Kondo model [10], the local moment is represented with fermionic spinons f_σ and the effective Hamiltonian is a resonant-level model with a hybridization $b = \langle \hat{b} \rangle_{MF} = \langle f_\sigma^\dagger c_{0\sigma} \rangle_{MF}$ (where \hat{b} is a bosonic operator). At this level, Kondo destruction corresponds to $b \rightarrow 0$, implying that the local moment is completely free and no longer entangled with the conduction band. Thus, such a static mean-field theory cannot reproduce the nonzero entanglement entropy that we find in the Kondo-destroyed phase. Our results can be understood, however, in terms of a bosonic operator $\hat{b}(\omega)$ that has a vanishing static component and give rises to a dynamical Kondo effect. Our results also imply that the Kondo-destroyed phase cannot be captured in variational quantum Monte Carlo studies of the Kondo lattice that treat b as a static variational parameter. It will be interesting to try and consider more general variational wave functions that can treat the Kondo-destroyed phase more accurately.

Kondo-destroyed quantum critical points have been invoked to understand the unconventional quantum criticality observed in experiments on heavy-fermion metals [50]. As a result of the failure of the Hertz-Millis-Moriya theory [52–54] of the spin-density-wave transition to describe the experimental data [51], the concept of local

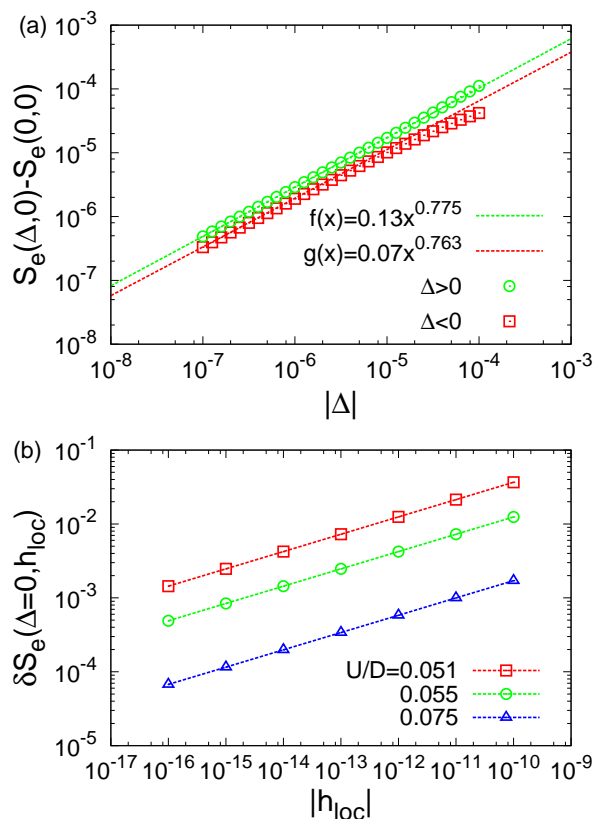


FIG. 8. (Color online) Critical behavior of the entanglement entropy S_e for the pseudogap Anderson model with $r = 0.6$, $\epsilon_d = -0.05D$, and $U \neq -2\epsilon_d$: (a) Shift in the zero-field entanglement entropy for $U = 0.055D$ on moving away from the quantum critical point into the local-moment phase ($\Delta < 0$) and the Kondo phase (Δ). Power-law fits to Eq. (38) yield $\tilde{\gamma} = 0.23(1)$. (b) Local-field-dependent part of the entanglement entropy δS_e vs h_{loc} at the critical hybridization width, for $U/D = 0.051, 0.055$, and 0.075 . The data are consistent with Eq. (11b) with $1/\delta_e = 0.2340(1)$.

quantum criticality [26] has been used to understand the energy-over-temperature scaling in the dynamic spin susceptibility, the presence of an additional energy scale, and a jump in the Fermi-surface volume. The theory of local quantum criticality is based on the extended-dynamical mean-field theory of the Kondo lattice [26], which finds that for sufficiently strong quantum fluctuations the Kondo effect is indeed destroyed at the antiferromagnetic QCP. The results of the present study imply that a continuous loss of entanglement is expected at the Kondo-breakdown QCPs believed to occur in certain heavy-fermion systems [55].

Our results might be tested using engineered realizations of some of the models, including single-electron transistors attached to ferromagnetic leads [28] and certain double-quantum-dot systems [31, 32]. Equation (32) shows that in the Kondo phase, knowledge of $\langle n_d \rangle$ and $\langle n_{d\uparrow} n_{d\downarrow} \rangle$ is sufficient to determine S_e . Since the charge

on a quantum dot can be measured using a variety of quantum point-contact techniques [56], and it is now becoming possible to probe double occupancy using optical spectroscopy techniques [57], there is a very exciting possibility of being able to extract the impurity entanglement entropy directly from experiments.

The remarkable simplicity of the variation of the impurity entanglement entropy near a Kondo-destruction QCP, as embodied in Eq. (10), can be attributed to the application of Eq. (1) with subsystem A containing just the impurity degrees of freedom and subsystem B encompassing just the host degrees of freedom. If one considered a different partition of the system in which host degrees of freedom were split between subsystems A and B , then S_e would probe entanglement within the host, which should be much more sensitive than impurity-host entanglement to details such as the number of conduction bands and/or the presence of bosonic baths. The critical behavior near impurity QCPs of entanglement entropy defined using alternative system partitions forms an interesting open question for future work.

VI. CONCLUSIONS

We have studied the quantum mechanical entanglement between a magnetic impurity and its environment in several models that feature critical destruction of the Kondo effect. In the Kondo-destroyed phase of each model studied, we have identified a term in the entanglement entropy varying with a critical exponent $\beta_e = 2\beta$, where β is the critical exponent governing the order parameter characterizing the quantum phase transition. In addition, we have established that the response of S_e to a local magnetic field gives rise to a part of the entanglement entropy that varies with a critical exponent $1/\delta_e = 2/\delta$, where δ is the critical exponent governing the response of the order parameter at the QCP to a local magnetic field. We have established very generally that in Kondo models, the ratio of the critical part of the entanglement entropy to the square of the order parameter depends only on the magnitude of the impurity spin, and not on the number of conduction channels or the presence of an additional bosonic bath. In nondegenerate Anderson models, this ratio is enhanced over its value in the $\text{Simp} = \frac{1}{2}$ Kondo model by a factor of the inverse of the impurity's local-moment fraction.

Our investigation has shown the absence of any universal behavior on approach to a Kondo-destruction quantum critical point from the Kondo (disordered) phase. In all variants of the Kondo model that we have considered, S_e remains pinned at its maximal value of $\ln(2S_{\text{imp}} + 1)$ throughout the Kondo phase. However, in Anderson models the presence of charge fluctuations introduces terms that depend on the values of $\langle n_{d\uparrow} + n_{d\downarrow} \rangle$ and $\langle n_{d\uparrow} n_{d\downarrow} \rangle$. We have shown that in the pseudogap Anderson model with a band exponent r on the range $0.55 \lesssim r < 1$, charge fluctuations produce a nonanalytic

leading variation of S_e near the QCP with a critical exponent that depends only on r . Away from particle-hole symmetry, S_e may rise on approach to the QCP from the Kondo side, producing a cusp peak in S_e precisely at the quantum phase transition. However, we also find situations in which the entanglement entropy decreases continuously, albeit nonanalytically, on passing from the Kondo phase to the local-moment phase.

VII. ACKNOWLEDGMENTS

We would like to thank Kenneth Evans, Márton Kormos, Jeremy McMinis, Doug Natelson, Qimiao Si, and

Aditya Shashi for useful discussions. This work was supported in part by the NSF Grant No. DMR-1309531, Robert A. Welch Foundation Grant No. C-1411, East-DeMarco fellowship, JQI-NSF-PFC, and LPS-CMTC (J.H.P.), by NSF Materials World Network Grant No. DMR-1107814 (T.C., C.W., and K.I.), and by the University of Florida REU Site in Materials Physics under NSF Grant No. DMR-1156737 (M.T.M. and J.S.).

-
- [1] A. Kitaev and J. Preskill, Phys. Rev. Lett. **96**, 110404 (2006); M. Levin and X.-G. Wen, *ibid.* **96**, 110405 (2006); P. Fendley, M. P. A. Fisher, and C. Nayak, J. Stat. Phys. **126**, 1111 (2007); H. Li and F. D. M. Haldane, Phys. Rev. Lett. **101**, 010504 (2008); H.-C. Jiang, Z. Wang and L. Balents, Nat. Phys. **8**, 902 (2012).
- [2] See, e.g., the reviews in P. Calabrese and J. Cardy, J. Phys. A: Math. Theor. **42**, 504005 (2009); G. Refael and J. E. Moore, *ibid.* **42**, 504010 (2009); E. Fradkin, *ibid.* **42**, 504011 (2009).
- [3] S. Sachdev, *Quantum Phase Transitions* (Cambridge Univ. Press, Cambridge, UK, 1999).
- [4] M. A. Nielsen and I. L. Chiang *Quantum Computation and Quantum Information* (Cambridge Univ. Press, Cambridge, UK, 2000).
- [5] I. Affleck, N. Laflorencie and E. S. Sorensen, J. Phys. A: Math. Theor. **42**, 504009 (2009).
- [6] A. Kopp and K. Le Hur, Phys. Rev. Lett. **98**, 220401 (2007).
- [7] K. Le Hur, P. Doucet-Beaupre and W. Hofstetter, Phys. Rev. Lett. **99**, 126801 (2007).
- [8] K. Le Hur, Ann. Phys. **323**, 2208 (2008).
- [9] A. C. Hewson, *The Kondo Problem to Heavy Fermions* (Cambridge University Press, Cambridge, UK, 1993).
- [10] D. Withoff and E. Fradkin, Phys. Rev. Lett. **64**, 1835 (1990).
- [11] R. Bulla, Th. Pruschke, and A. C. Hewson, J. Phys.: Condens. Matter **9**, 10463 (1997).
- [12] C. Gonzalez-Buxton and K. Ingersent, Phys. Rev. B **57**, 14254 (1998).
- [13] K. Ingersent and Q. Si, Phys. Rev. Lett. **89**, 076403 (2002).
- [14] L. Fritz and M. Vojta, Phys. Rev. B **70**, 214427 (2004).
- [15] I. Schneider, L. Fritz, F. B. Anders, A. Benlagra, and M. Vojta, Phys. Rev. B **84**, 125139 (2011).
- [16] M. T. Glossop, S. Kirchner, J. H. Pixley, and Q. Si, Phys. Rev. Lett. **107**, 076404 (2011).
- [17] J. H. Pixley, S. Kirchner, K. Ingersent, and Q. Si, Phys. Rev. Lett. **109**, 086403 (2012).
- [18] F. Zamani, T. Chowdhury, P. Ribeiro, K. Ingersent, and S. Kirchner, Phys. Status Solidi B **250**, 547 (2013).
- [19] A. M. Sengupta, Phys. Rev. B **61**, 4041 (2000).
- [20] L. Zhu and Q. Si, Phys. Rev. B **66**, 024426 (2002).
- [21] G. Zaránd and E. Demler, Phys. Rev. B **66**, 024427 (2002).
- [22] M. Kirčan and M. Vojta, Phys. Rev. B **69**, 174421 (2004).
- [23] M. T. Glossop and K. Ingersent, Phys. Rev. Lett. **95**, 067202 (2005).
- [24] M. T. Glossop and K. Ingersent, Phys. Rev. B **75**, 104410 (2007).
- [25] J. H. Pixley, S. Kirchner, K. Ingersent, and Q. Si, Phys. Rev. B **88**, 245111 (2013).
- [26] Q. Si, S. Rabello, K. Ingersent, and J. L. Smith, Nature (London) **413**, 804 (2001).
- [27] Q. Si, S. Rabello, K. Ingersent, and J. L. Smith, Phys. Rev. B **68**, 115103 (2003).
- [28] S. Kirchner, L. Zhu, Q. Si and D. Natelson, Proc. Natl. Acad. Sci. USA **102**, 18824 (2005).
- [29] M. Vojta and R. Bulla, Phys. Rev. B **65**, 014511 (2001).
- [30] L. Fritz and M. Vojta, Rep. Prog. Phys. **76**, 032501 (2013).
- [31] L. G. G. V. DiasdaSilva, N. P. Sandler, K. Ingersent, and S. E. Ulloa, Phys. Rev. Lett. **97**, 096603 (2006).
- [32] L. G. G. V. DiasdaSilva, K. Ingersent, N. P. Sandler, and S. E. Ulloa, Phys. Rev. B **78**, 153304 (2008).
- [33] K. G. Wilson, Rev. Mod. Phys. **47**, 773 (1975).
- [34] R. Bulla, T. A. Costi, and T. Pruschke, Rev. Mod. Phys. **80**, 395 (2008).
- [35] R. Bulla, N. H. Tong, and M. Vojta, Phys. Rev. Lett. **91**, 170601 (2003).
- [36] R. Bulla, H. J. Lee, N. H. Tong, and M. Vojta, Phys. Rev. B **71**, 045122 (2005).
- [37] Figure 30(a) of Ref. 12 shows a line of QCPs occurring for $0 < r < r_{\max}$. Reference 15 shows that this picture is incorrect, and that there is instead weak renormalization-group flow along the phase boundary toward a unique particle-hole-symmetric QCP.
- [38] H. Spohn and R. Dümke, J. Stat. Phys. **41**, 495 (1985).
- [39] S. Kirchner and Q. Si, Phys. Rev. Lett. **100**, 026403 (2008).
- [40] Although it does not specifically identify the spontaneous-symmetry-breaking part of the entanglement entropy, Ref. 7 does note that on entry to the localized phase of the sub-Ohmic spin-boson model with $1/2 < s < 1$, the entanglement entropy decreases according to an exponent $\nu(1-s)$ that coincides with 2β , in agreement with our Eqs. (11a) and (12a).

- [41] E. M. Nica, K. Ingersent, J.-X. Zhu, and Q. Si, Phys. Rev. B **88**, 014414 (2013).
- [42] M. Cheng and K. Ingersent, Phys. Rev. B **87**, 075145 (2013).
- [43] D. Larsson and H. Johannesson, Phys. Rev. Lett. **95**, 196406 (2005).
- [44] For $r^* \simeq 3/8 < r < \frac{1}{2}$, the pseudodap Anderson and $S_{\text{imp}} = \frac{1}{2}$ Kondo models feature separate symmetric and asymmetric QCPs having distinct critical exponents. This accounts for the difference between the $r = 0.4$ values of β quoted in Table I and in connection with the Anderson model.
- [45] D. E. Logan and M. T. Glossop, J. Phys.: Condens. Matter **12**, 985 (2000).
- [46] T. Chowdhury and K. Ingersent, Phys. Rev. B **91**, 035118 (2015). This work shows that the charge-susceptibility exponent can be written $\tilde{\gamma} = 2 - \nu$ in terms of the correlation-length exponent ν , which describes the vanishing of a crossover temperature $T^* \propto |\Delta|^\nu$ on approach to the quantum-critical point.
- [47] The large- Γ limit of the local-moment fraction is $f = \frac{1}{2}$, and not $f = 2/3$ corresponding to the effective degeneracy of three impurity configurations $|0\rangle$, $|\uparrow\rangle$, and $|\downarrow\rangle$. This is because for $\Gamma \gg |\epsilon_d|, D$, the many-body ground state contains equal admixtures of $(c_{0\uparrow}^\dagger|0\rangle + |\uparrow\rangle)/\sqrt{2}$ and $(c_{0\downarrow}^\dagger|0\rangle + |\downarrow\rangle)/\sqrt{2}$.
- [48] K. Ingersent, unpublished.
- [49] The locations Γ/Γ_c of extrema in $S_e(h_{\text{loc}} = 0)$, as well as the extremal values themselves, are weakly dependent on the Wilson discretization parameter Λ employed in the NRG calculations. The NRG results quoted in Section IV were computed for $\Lambda = 9$. We have determined for $r = 0.6$, $\epsilon_d = -0.05D$, and $U = 0.051D$, that reducing Λ from 9 to 3 shifts the peak in $S_e(h_{\text{loc}} = 0)$ from $\Delta = 5.1 \times 10^{-5}$ to $\Delta = 6.0 \times 10^{-5}$. That this shift is to a slightly *larger* $|\Delta|$ value provides evidence that the displacement of the peak away from the quantum critical point is not merely an artifact of the NRG, and that a nonzero displacement would survive in the continuum limit $\Lambda \rightarrow 1$.
- [50] P. Gegenwart, Q. Si, and F. Steglich, Nature Physics **4**, 186 (2008).
- [51] P. Coleman et al., J. Phys. Cond. Matt. **13**, R723 (2001).
- [52] J. A. Hertz, Phys. Rev. B **14**, 1165 (1976).
- [53] A. J. Millis, Phys. Rev. B **48**, 7183 (1993).
- [54] T. Moriya, *Spin Fluctuations in Itinerant Electron Magnetism*, 44–81 (Springer, Berlin, 1985).
- [55] Q. Si, J. H. Pixley, E. Nica, S. J. Yamamoto, P. Goswami, R. Yu, and S. Kirchner, J. Phys. Soc. Jpn. **83** 061005 (2014).
- [56] T. Ihn, *Electronic quantum transport in mesoscopic semiconductor structures* (Springer-Verlag, New York, USA, 2004).
- [57] C. Latta, et al., Nature **474**, 627 (2011).